

Lattice modes in molecular crystals measured with nuclear inelastic scattering

V. G. Kohn,^{1,*} A. I. Chumakov,^{1,2,†} and R. Rüffer²

¹Russian Research Center “Kurchatov Institute”, 123182, Moscow, Russia

²European Synchrotron Radiation Facility BP220, F-38043 Grenoble, France

(Received 28 July 2005; revised manuscript received 30 January 2006; published 29 March 2006)

We reveal an important property of nuclear inelastic scattering in a molecular crystal with well-separated lattice and molecular modes: The presence of the molecular modes does not change the shape but merely rescales the lattice part of the energy dependence of nuclear inelastic scattering. Therefore, the density of states (DOS) of the lattice vibrations can be properly derived even from the lattice part of nuclear inelastic scattering alone. In this case, one has to substitute the mean recoil energy of a nucleus by the effective recoil energy of the molecule. In first approximation, the ratio of the recoil energies is close to the ratio of the nuclear and molecular masses. More precisely, it is given by the relative area of the lattice part in the entire DOS. The theoretical analysis is verified with numerical calculations for a model DOS and with the experimental data for the decamethyl ferrocene molecular crystal. More generally, the analysis is valid for any region of nuclear inelastic scattering around the central elastic peak with sufficiently narrow lines beyond it. Therefore, the demonstrated property of nuclear inelastic scattering allows for a much shorter measuring time in studies of lattice modes in molecular crystals, low-energy molecular modes in proteins, and in investigations of glass dynamics with molecular probes.

DOI: [10.1103/PhysRevB.73.094306](https://doi.org/10.1103/PhysRevB.73.094306)

PACS number(s): 63.20.-e, 76.80.+y, 07.85.-m

I. INTRODUCTION

Synchrotron radiation sources of the third generation provide well-collimated beams of hard x rays with extremely high spectral density, up to 10^{14} photons/eV/sec. These properties gave rise to a number of new techniques related to excitation of nuclear levels with long (~ 100 ns) lifetime and, correspondingly, with very narrow (\sim neV) energy width. One of the recent techniques is nuclear inelastic scattering (NIS), which allows for studies of atomic vibrations for isotopes with relatively low energies of nuclear excited states.¹⁻⁴

A nuclear inelastic scattering experiment monitors the yield of a delayed nuclear interaction—scattering or absorption—as a function of energy of incident x rays varied around the energy of the nuclear resonance. The accompanied prompt electronic scattering is separated using the pulse structure of synchrotron radiation and the relatively long lifetime of nuclear excitation. The incident radiation is monochromatized down to an energy width of about 1 meV. When the products of nuclear absorption are detected, the monitored process is nuclear inelastic absorption. By definition, it is spatially incoherent over various nuclei. Furthermore, even if the products of nuclear scattering are detected, the process is also properly described by the theory of spatially incoherent scattering.⁵⁻⁹

In practice, the measured energy spectrum is proportional to the probability of incoherent nuclear scattering for all energies except for the central elastic peak, where the yield of scattering is saturated due to the high cross section of elastic scattering. In addition, the saturation of the elastic peak is further enhanced because the NIS signal cannot be collected during a short but finite time interval after the incident synchrotron radiation pulse. The time gating decreases the relative weight of the central peak, because the time structure of

elastic incoherent scattering is speeded up compared to the simple exponential time evolution due to a speedup effect in nuclear forward scattering. See the Appendix for the extended theory of elastic incoherent scattering and for the details of the speedup effect.

According to the theory of incoherent nuclear inelastic scattering, the probability of scattering is entirely determined by the partial (i.e., for resonant atoms) density of phonon states projected onto the direction of the incident beam. For shortness, here we call this function the density of states (DOS). Determination of the DOS is the main aim in processing data of nuclear inelastic scattering.

After verification of the principles of nuclear inelastic scattering with elementary solids,^{1,2,10} research activity on the new technique developed rapidly in the direction of complex systems, in particular molecular crystals and proteins.¹¹⁻¹⁴ In these objects, atomic vibrations may be decomposed into the continuous spectrum of lattice phonons and narrow bands of local molecular modes. The presence of two types of vibrational dynamics poses to theory important questions concerning the interplay of various modes in the energy dependence of nuclear inelastic scattering. The reason is that the total probability of inelastic scattering is not a linear combination of the partial probabilities related to various modes of the density of states. Therefore, even if the vibrational modes are well separated in the DOS, they are mixed in the energy dependence of nuclear inelastic scattering.

Recently we analyzed the influence of the lattice phonons on the appearance of molecular modes in the energy dependence of nuclear inelastic scattering.¹⁵ We found that near the molecular peaks, the probability of a nuclear interaction can be treated as combined nuclear-molecular resonance inelastic scattering. This feature allows for an independent investigation of lattice phonons for different coexisting phases in heterogeneous samples.

In this paper, we consider an opposite question: the influence of the high-energy molecular modes on the low-energy lattice part in the energy dependence of nuclear inelastic scattering. We show that the presence of the molecular modes practically does not change the shape of the lattice part of the curve but mainly rescales it. Therefore the influence of the molecular modes is reduced to a scaling factor, and the lattice part of the DOS can be derived from the lattice part of nuclear inelastic scattering alone.

Because of elastic peak saturation, the measured energy spectrum cannot be normalized to a unit area. The proper normalization is achieved using the first moment of the energy spectrum.² According to Lipkin's sum rules,¹⁶ the first moment is equal to the recoil energy of a free nucleus, $E_R = (\hbar k)^2/2m$, where $k=|\mathbf{k}|$, \mathbf{k} is the wave vector of the incident photon, m is the mass of the resonant nucleus, and \hbar is the reduced Planck's constant. Compared to the area (zero-moment) normalization, the use of the first moment enhances the significance of the high-energy regions in the energy spectrum. Therefore, the energy spectrum should be measured far beyond the actual region of interest. This mismatch is particularly large in studies of the lattice phonons of molecular crystals and in measurements of collective modes of glasses using probe molecules.¹⁷ The main interest in these studies is focused on the low-energy region, whereas for proper normalization the energy spectrum has to be measured including all high-energy peaks of molecular modes.

It is evident that for processing the lattice part of NIS alone the value of the recoil energy has to be reevaluated. One can intuitively understand what the recoil energy required is. Discarding the molecular degrees of freedom is equivalent to treating the molecule as a rigid body. In this model, the resonant atom is not allowed to move relative to the rest of the molecule. Therefore, recoil cannot be accepted by the resonant atom individually, but is delivered to the entire molecule. Thus, one can guess that in processing the lattice part of nuclear inelastic scattering alone, one has to substitute the recoil energy of a free nucleus by that of a free molecule. The ratio of the recoil energies is obviously equal to the ratio of the nuclear and molecular masses. We show that although this estimation is indeed a very good first approximation, it is not exact. More precisely, the ratio is given by the relative area of the lattice part in the entire DOS.

We note that such an analysis is valid not only for the lattice part, but also for any region of nuclear inelastic scattering around the central elastic peak with sufficiently narrow and well-separated peaks beyond it. In all such cases, the demonstrated property of nuclear inelastic scattering allows for a shorter measuring time. This is applicable for a wide range of complex solids such as molecular crystals and proteins.

The paper consists of six sections. In Sec. II, we start with general equations. In Sec. III, we analyze the energy dependence of the lattice part of nuclear inelastic scattering in the presence of the molecular modes. In Sec. IV, we confirm the analysis by numerical calculations for a model DOS. In Sec. V, the method is verified with experimental data on nuclear inelastic scattering for decamethyl ferrocene molecular crystal. In Sec. VI, we discuss the application of the method.

II. GENERAL EQUATIONS

For simplicity we assume equivalent positions and identical vibrational properties for all atoms with the resonant nuclei. Neglecting the narrow width of the nuclear resonance, the frequency dependence of the normalized probability density of nuclear incoherent inelastic scattering $S(\mathbf{k}, \omega)$ is determined by the Fourier transformation of the intermediate self-correlation function $F(\mathbf{k}, t)$ (Refs. 5 and 6):

$$S(\mathbf{k}, \omega) = \int \frac{dt}{2\pi} \exp(-i\omega t) F(\mathbf{k}, t). \quad (1)$$

Here ω is the frequency shift of the incident photon from the frequency ω_0 of nuclear resonance; \mathbf{k} is the wave vector of the incident photon. The function

$$F(\mathbf{k}, t) = \langle \exp[-i\mathbf{k} \cdot \mathbf{u}(0)] \exp[i\mathbf{k} \cdot \mathbf{u}(t)] \rangle \quad (2)$$

describes the correlation of nuclear positions \mathbf{u} in two moments separated by the time interval t . The angular brackets denote both quantum-mechanic and thermodynamic averaging. In harmonic approximation this function can be written as⁶

$$F(\mathbf{k}, t) = f(\mathbf{k}) \exp[M(\mathbf{k}, t)], \quad f(\mathbf{k}) = \exp[-M(\mathbf{k}, 0)], \quad (3)$$

where $f(\mathbf{k})$ is the Lamb-Mössbauer factor and

$$M(\mathbf{k}, t) = \int d\omega \exp(i\omega t) \frac{\omega_R g(\mathbf{k}, |\omega|)}{\omega [1 - \exp(-\beta\omega)]}. \quad (4)$$

Here $g(\mathbf{k}, \omega)$ is the partial (for the atoms with the resonant nucleus) density of states projected onto the direction of the incident beam \mathbf{k} , $\omega_R = E_R/\hbar$, $\beta = \hbar/(k_B T)^{-1}$, k_B is the Boltzmann constant, and T is the temperature. The density of states $g(\mathbf{k}, \omega)$ is normalized to unity. To shorten, we omit the \mathbf{k} argument in the formulas below.

Equations (1)–(4) show that for given experimental conditions (temperature of the sample, energy of the incident radiation, and mass of the resonant nucleus), the probability density of nuclear incoherent scattering $S(\omega)$ is uniquely determined by the density of states $g(\omega)$. It is easy to show⁶ that the DOS can also be uniquely derived from a given probability density of nuclear scattering. Furthermore, the first moment of the probability density of nuclear incoherent scattering is uniquely related to the DOS normalization:

$$\begin{aligned} \int_{-\infty}^{\infty} d\omega \omega S(\omega) &= \lim_{\varepsilon \rightarrow 0} \int d\omega \int \frac{dt}{2\pi} \exp(-i\omega t - \varepsilon|t|) \omega F(t) \\ &= \lim_{\varepsilon \rightarrow 0} \int \frac{dt}{2\pi i} \frac{d}{dt} [\exp(-\varepsilon|t|) F(t)] \\ &\quad \times \int d\omega \exp(-i\omega t) \\ &= \left(\frac{dF(t)}{idt} \right)_{t=0} \\ &= \left(\frac{dM(t)}{idt} \right)_{t=0} \end{aligned}$$

$$\begin{aligned}
&= \omega_R \int d\omega \frac{g(|\omega|)}{[1 - \exp(-\beta\omega)]} \\
&= \omega_R \int_0^\infty d\omega g(\omega). \quad (5)
\end{aligned}$$

Let us consider a lattice-phonon part of the energy dependence of nuclear inelastic scattering around the central elastic peak, which excludes all higher-energy molecular modes. To shorten, we call this part the “truncated spectrum.” For the moment, let us suppose that the presence of the higher-energy molecular modes does not affect the shape of the truncated spectrum. Then, because of the unique relation between the probability density of nuclear incoherent scattering and the DOS, the density of the lattice phonon states can be correctly determined from the truncated spectrum after its appropriate normalization. The proper normalization coefficient is given by Eq. (5): The first moment of the truncated spectrum should be equal to the recoil energy of a free nucleus multiplied by the relative area of the lattice DOS. On the other hand, the proper normalization of the truncated spectra can be achieved simply by the renormalization of the recoil energy considering the lattice DOS normalized by unity as it was pointed above.

The normalization relation (5) is obtained using analytical properties of the Fourier transformation. This approach does not reveal a relative role of multiphonon terms, which we will need in the analysis below. In order to estimate the importance of the multiphonon contributions, we calculate the normalization relation, keeping only the single-phonon term S_1 of the probability of inelastic scattering. In this case the calculations can be performed with the variable integration limits:

$$\begin{aligned}
\int_{-a}^a d\omega \omega S_1(\omega) &= f \int_{-a}^a d\omega \omega \int \frac{dt}{2\pi} \exp(-i\omega t) M(t) \\
&= \omega_R f \int_{-a}^a d\omega \frac{g(|\omega|)}{[1 - \exp(-\beta\omega)]} \\
&= \omega_R f \int_0^a d\omega g(\omega). \quad (6)
\end{aligned}$$

At the limit of $a \rightarrow \infty$, the first moment of the single-phonon term (6) is less than that of the total spectrum (5) by the Lamb-Mössbauer factor $f < 1$. The difference obviously should be attributed to the multiphonon contributions, which were properly accounted for in Eq. (5) but not in Eq. (6).

III. ANALYTICAL ESTIMATIONS

We have shown that the lattice DOS can be correctly derived from the truncated energy spectrum after the proper renormalization of the recoil energy if the presence of the molecular modes does not change the shape of the lattice part of the energy spectrum. In this section, we analyze analytically the validity of the assumption on a simple model DOS.

We consider the density of states $g(\omega) = g_c(\omega) + g_m(\omega)$ composed of the collective lattice part $g_c(\omega)$ with an area of

A_c and only a single peak of molecular mode $g_m(\omega)$:

$$g_m(\omega) = A_m p(\omega - \omega_m), \quad p(\omega) \xrightarrow{|\omega| \rightarrow \infty} 0,$$

$$\int d\omega p(\omega) = 1, \quad A_m = 1 - A_c. \quad (7)$$

In this case the probability density of nuclear inelastic scattering can be written as

$$\begin{aligned}
S(\omega) &= f \int \frac{dt}{2\pi} \exp(-i\omega t) \exp[M_c(t)] \left[1 + \sum_{n=1}^{\infty} \frac{1}{n!} [M_m^{(+)}(t) \right. \\
&\quad \left. + M_m^{(-)}(t)]^n \right], \quad (8)
\end{aligned}$$

where

$$M(t) = M_c(t) + M_m(t) = M_c(t) + M_m^{(+)}(t) + M_m^{(-)}(t),$$

$$M_c(t) = \int d\omega \exp(i\omega t) \frac{\omega_R g_c(|\omega|)}{\omega [1 - \exp(-\beta\omega)]},$$

$$M_m^{(+)}(t) = \exp(i\omega_m t) m(t),$$

$$m(t) = \frac{\omega_R A_m}{\omega_m [1 - \exp(-\beta\omega_m)]} P(t),$$

$$M_m^{(-)}(t) = \exp(-i\omega_m t) \exp(-\beta\omega_m) m(t). \quad (9)$$

Here $P(t)$ is the Fourier image of $p(\omega)$. Evaluating the M_m contribution in Eqs. (8) and (9), we substituted the frequency variable in the Bose-occupation factor and in the inverse frequency by the molecular mode frequency ω_m . This approximation is precise enough if ω_m is much bigger than the width of the molecular peak.

Now we select only the terms which contribute to the low-energy part of the spectrum $S_c(\omega)$ around the region of the lattice vibration. These are the terms free of the exponentials $\exp(\pm i l \omega_m t)$ with $l > 0$ —i.e., the terms with simultaneous excitation and annihilation of an equal number of molecular vibrations. Then the expansion in Eq. (8) contains only even $n = 2k$ and can be reduced to

$$\begin{aligned}
S_c(\omega) &= f \int \frac{dt}{2\pi} \exp(-i\omega t) \exp[M_c(t)] \left[1 + \sum_{k=1}^{\infty} \frac{[C_m(t)]^{2k}}{2^{2k} (k!)^2} \right] \\
&= f \int \frac{dt}{2\pi} \exp(-i\omega t) \exp[M_c(t)] I_0(C_m(t)), \quad (10)
\end{aligned}$$

where $I_0(z)$ is the modified Bessel function of the first kind and

$$C_m(t) = 2 \exp(-\beta\omega_m/2) m(t) = \frac{\omega_R A_m}{\omega_m \sinh(\beta\omega_m/2)} P(t). \quad (11)$$

Equation (10) gives the probability density of nuclear incoherent scattering in the central part of the energy spectrum.

It includes all single-phonon and multiphonon terms of the lattice modes. It also includes that part of the multiphonon terms of the molecular modes which contributes to the central part of the energy spectrum. The contribution of the multiphonon terms of the molecular modes is described by the Bessel function with the argument proportional to the Fourier image $P(t)$ of the molecular peak. The characteristic width of this peak is usually much smaller than the frequency spectrum of the lattice vibrations. For their Fourier images the opposite relation is valid; i.e., the width of the function $P(t)$ is much larger than that of $M_c(t)$. Therefore, in the integral (10) we can approximately substitute the function $P(t)$ by its constant value at zero time $P(0)$:

$$S_c(\omega) \approx f_m I_0(C_m(0)) \left[f_c \int \frac{dt}{2\pi} \exp(-i\omega t) \exp[M_c(t)] \right]. \quad (12)$$

Here we expressed the Lamb-Mössbauer factor f in the factorized form $f = f_c f_m$, where $f_c = \exp[-M_c(0)]$ is the lattice fraction of the entire Lamb-Mössbauer factor and the molecular fraction f_m is

$$f_m = \exp[-M_m(0)] = \exp\left(-\frac{\omega_R A_m}{\omega_m \tanh(\beta\omega_m/2)}\right). \quad (13)$$

The expression in the large square brackets of Eq. (12) gives the normalized probability density of nuclear scattering by lattice modes [compare to Eqs. (1)–(3)]. Thus, we see that the energy dependence of nuclear inelastic scattering in the central energy region has a shape close to the exact energy spectrum of the lattice modes. The influence of the molecular modes is reduced to a scaling constant composed of two factors f_m and $I_0(C_m(0))$.

The first factor $f_m < 1$ decreases the area and first moment of the energy spectrum of lattice modes. It is a strict constant, because it comes from the exact solution (10) and is thus not bounded by the assumption made in the derivation of approximation (12). According to Eq. (13), this is a first-order correction with respect to the height of the molecular peaks. This is the same correction that causes the already discussed difference between Eqs. (5) and (6): The central part of the spectrum contains all the multiphonon terms of the lattice modes, whereas many of the multiphonon terms of the molecular modes are located beyond the truncated spectrum. Therefore, the multiphonon contributions of the lattice modes compensate for the lattice fraction of the Lamb-Mössbauer factor f_c , whereas the molecular fraction f_m remains noncompensated.

Some multiphonon terms, however, do contribute to the low-energy lattice part. The relevant contribution is described by the second factor $I_0(C_m(0)) > 1$. It partly compensates for the decrease caused by the first factor f_m . The second correction is a constant only under the assumption of essentially narrow molecular modes. However, it is the second-order correction with respect to the height of the molecular peaks, because it includes not all but only selected multiphonon terms with an even number of excited and annihilated phonons.

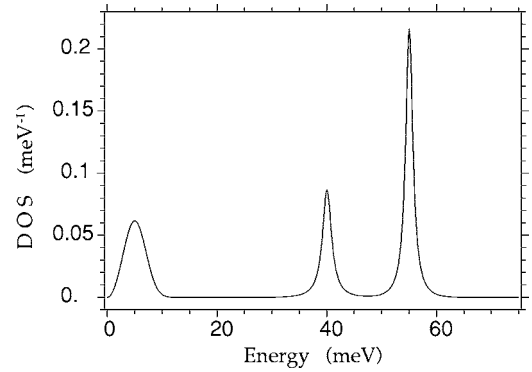


FIG. 1. The model DOS with the low-energy lattice part and two molecular peaks at 40 and 55 meV.

IV. NUMERICAL SIMULATION

We have shown analytically that the presence of a molecular mode does not change the shape of the central part of the energy spectrum if the molecular mode has a sufficiently narrow energy distribution. The next step is to check the reality of this approximation in exact numerical calculations for a typical energy spectrum with the finite linewidths of the molecular modes. In this section, we perform this test with a model DOS.

The model DOS is shown in Fig. 1. It contains the collective lattice part $g_c(\omega)$ in the low-energy region and two peaks of molecular modes. The lattice part is simulated by the function

$$g_c(\omega) = g_{cm} x^2 \exp\left(\frac{2}{3}(1-x^3)\right), \quad x = \frac{\omega}{\omega_{\max}}. \quad (14)$$

It has a maximum value g_{cm} at $\omega = \omega_{\max} = 5$ meV. The area of the lattice part of the DOS is 0.30. The molecular peaks are modeled by a product of the Lorentz and Gauss distributions with a width ratio of 1/5, respectively. The broader Gaussian is used for a reduction of the long tails in the Lorentz function. The full width at half maximum (FWHM) of the peaks at 40 and 55 meV are 2.0 and 1.6 meV, respectively. The total area of the molecular part of the DOS is 0.70; thus, the entire DOS is normalized to unity.

Figure 2 shows the energy spectrum of nuclear inelastic

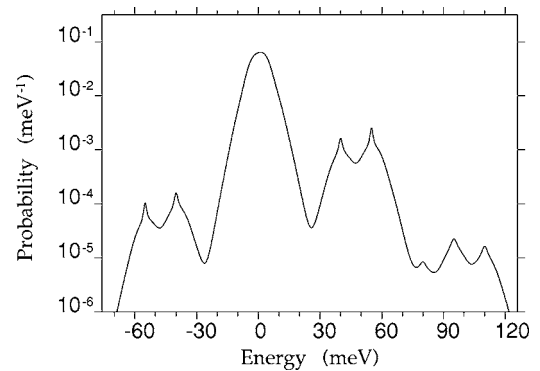


FIG. 2. The normalized probability density of nuclear inelastic scattering calculated from the model DOS.

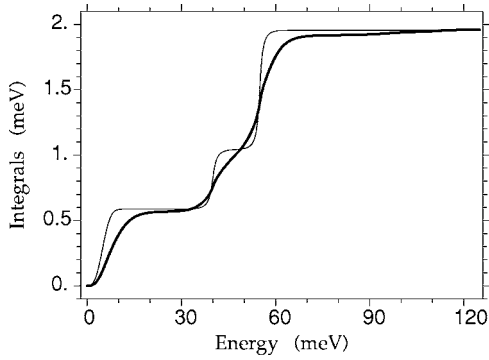


FIG. 3. Comparison of the DOS integral and the moment integral with variable integration limits. The exact definition of the functions is given in the text. The thin line is the DOS integral multiplied by E_R . The thick line is the integral of the first moment of the spectrum.

scattering calculated from the model DOS for the temperature 200 K and ^{57}Fe nucleus. The δ function of the central elastic peak is omitted. The spectrum contains the single-phonon contributions of the molecular modes at the corresponding energies in both the phonon-annihilation (left) and phonon-creation (right) parts. In addition, for the phonon-creation part it shows the three double-phonon peaks at 80, 95, and 110 meV. The corresponding peaks at the phonon-annihilation part are not shown, because they are very small.

Before proceeding with the reverse calculations of the lattice DOS from the truncated energy spectrum, we analyze the relation between the normalization of the DOS and energy spectrum. Figure 3 shows the integral of the DOS area multiplied by $E_R=1.956$ meV and the integral of the first moment of the spectrum as a function of the integration limits. To shorten, we will call these functions as the DOS integral and the moment integral, respectively. The mathematical expressions for these functions are given by the left and right sides of Eq. (5) if one replaces ω by E' , ω_R by E_R , and the infinite limit by finite limit E .

According to Eq. (5) the two curves should approach the same value of E_R at $E \rightarrow \infty$. The DOS integral experiences a sharp rise in the energy regions of nonzero DOS, and it is practically constant in between these regions. The moment integral approximately follows the same trend. However, it varies much more smoothly, because the addition of the multiphonon processes widens the energy regions of nonzero inelastic scattering. For instance, at $E=75$ meV the moment integral still does not reach the proper normalization level. Only above 120 meV, after account of the two-phonon molecular peaks is it sufficiently close to the exact value of E_R .

A similar trend is observed at $E=25$ meV. Here the DOS integral includes already the entire lattice part of the DOS and, therefore, is equal to $0.3E_R$, whereas the moment integral has a lower value of $0.291E_R$. The difference hardly can be explained by the missing multiphonon contributions of the lattice modes because, according to Fig. 2, they almost vanish at this energy. The true reason for the discrepancy is the renormalization of the lattice part of the spectrum discussed in the previous section: Because of the presence of the molecular modes, the lattice part of the spectrum is

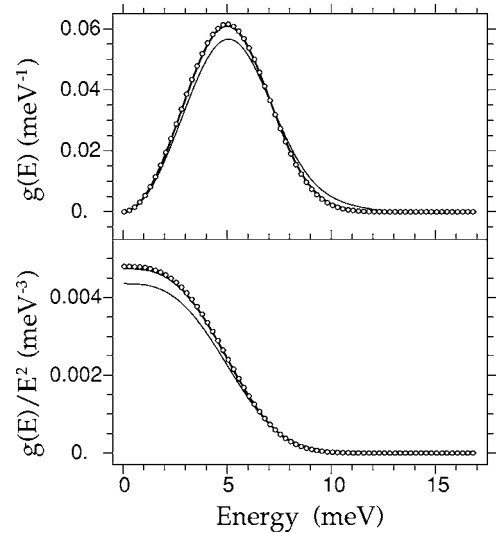


FIG. 4. Comparison of the initial DOS $g(E)$ (open circles) and those obtained after reverse calculations of the DOS from the truncated energy spectrum. The thick line shows the DOS recalculated from the truncated and then properly renormalized energy spectrum so that its first moment is equal to $0.3E_R$. The thin line shows the DOS calculated from the truncated spectrum obtained without renormalization from the total normalized energy spectrum. In the latter case, the first moment of the truncated spectrum is equal $0.291E_R$. In both cases the spectrum was truncated beyond the energy region of $(-25, 25)$ meV. The bottom panel shows the corresponding functions $g(E)/E^2$ in order to emphasize the low-energy region.

scaled by a factor similar to $f_m I_0(C_m(0))$ in the case of one molecular peak.

We truncated the energy spectrum of Fig. 2 beyond the energy region $|E| < 25$ meV and normalized it so that the first moment of the truncated spectrum is equal to the effective recoil energy $A_c E_R = 0.3E_R$. After that, the reverse calculations of the lattice DOS were performed according to the conventional procedure⁸ using the recoil energy E_R .¹⁸ The derived DOS is compared to the initial one in Fig. 4. In order to check the consistency of the results in the low-energy region, we also show the function $g(E)/E^2$. The difference between the initial and recalculated DOS, if any, is negligible. Thus, the presence of the molecular modes causes no notable changes in the shape of the lattice part of the energy spectrum of inelastic scattering.

In order to illustrate the importance of the correct normalization, we repeat the calculations with the deliberately wrong parameter of the effective recoil energy $0.291E_R$, which is the first moment of the lattice part in the total normalized energy spectrum of inelastic scattering. In other words, we do not correct for the scaling of the truncated spectrum by the factor caused by the presence of the molecular modes. Figure 4 shows that the calculated DOS significantly differs from the initial one. Thus, even a 3% mistake in the normalization can cause notable errors in the shape of the calculated DOS.

V. EXPERIMENT

Numerical calculations show that the presence of a few narrow local modes located at sufficiently high energies in-

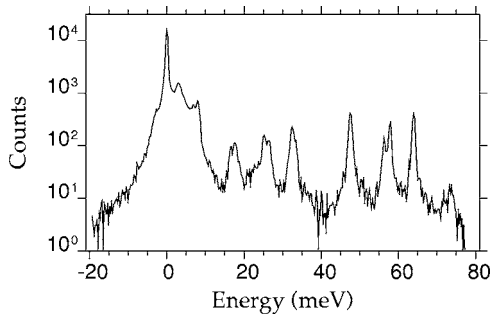


FIG. 5. The energy dependence of nuclear inelastic scattering for decamethyl ferrocene powder measured at 22.3 K.

deed does not change much the shape of the central part of the energy spectrum. Therefore, the reverse calculation of the lattice DOS from the truncated spectrum allows for good agreement of the results with the initial DOS. In practice, the energy spectrum could contain a larger number of the molecular modes; the width of the molecular modes could be larger, and the modes could be located closer to the lattice continuum. In this section, we verify the stability of the proposed approach with the example of the experimental data for the decamethyl ferrocene $\text{FeC}_{20}\text{H}_{30}$ molecular crystal.

The measurements were performed at the Nuclear Resonance beamline¹⁹ at the European Synchrotron Radiation Facility using the inelastic spectrometer²⁰ with 0.5 meV energy resolution. The details of the experimental setup and the method can be found elsewhere.⁴ The decamethyl ferrocene sample was enriched in the resonance ^{57}Fe isotope up to 95%. The sample was in powder form. The measurements were performed at 22.3 K.

Figure 5 shows the measured energy dependence of nuclear inelastic scattering. It contains the central elastic peak, the collective lattice modes within the $|E| < 13$ meV energy region, and about ten molecular peaks spreading in energy from 17 up to 74 meV. According to the Bose statistics, the phonon annihilation part ($E < 0$) is almost absent at the low-temperature conditions.

The total density of vibrational states calculated from the experimental data is shown in Fig. 6. A unit cell of the decamethyl ferrocene crystal lattice contains four molecules.²¹ Thus, the lattice part of the DOS should have three acoustic and nine optical modes. The lattice part of the DOS ($|E| < 10$ meV) shows the Debye-like parabolic rise of the acous-

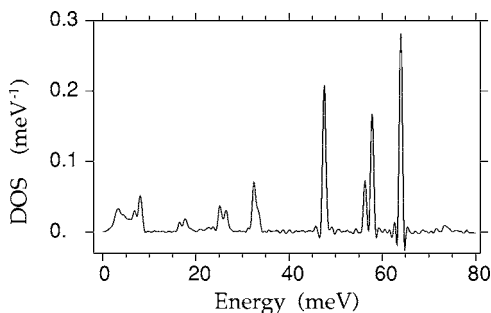


FIG. 6. The density of vibrational states for decamethyl ferrocene calculated from the entire energy spectrum.

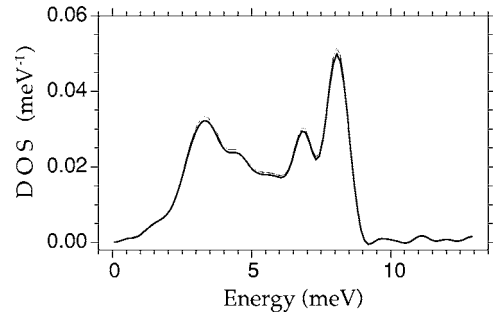


FIG. 7. Comparison of lattice parts of the DOS calculated from the entire energy spectrum (thin line) and from the spectrum truncated beyond the energy interval of $(-13, 13)$ meV (thick line).

tic lattice modes from zero to 3 meV and several peaks of the optical lattice modes at 3.5, 4.5, 7, and 8 meV.

In the extreme of long-wavelength acoustic vibrations, the molecule moves as a rigid body without displacement of individual atoms relative to each other. In molecular crystals with several molecules in a unit cell, this approximation works well even for lattice modes up to the boundaries of the Brillouin zone, because the corresponding wavelength is still larger than the molecular size. Within the rigid-body approximation, one can easily show that the relative contribution of the lattice phonons to the entire DOS is equal to the ratio of the nuclear and molecular masses.^{12,13} For the decamethyl ferrocene molecular crystal, the total area of the lattice part of the DOS is 0.178(1). This value is very close to 0.174, which is the mass ratio of the resonant isotope ^{57}Fe and the $^{57}\text{FeC}_{20}\text{H}_{30}$ molecule. Thus, the decamethyl ferrocene is a sufficiently rigid molecule. With lattice modes, it moves as a rigid body with only about 2% of the motional energy embedded into molecular deformation.

We truncated the measured energy spectrum of nuclear inelastic scattering of Fig. 5 beyond the energy range of $|E| < 13$ meV and renormalized it according to the effective recoil energy $0.178E_R$. After that, the reverse calculations of the lattice DOS were performed according to the conventional procedure using the nucleus recoil energy E_R . The obtained DOS is shown in Fig. 7. The two lattice DOS calculated from the total and truncated energy spectra are basically indistinguishable from each other. This evidences the stability of the proposed approach.

VI. DISCUSSION

We have shown that the lattice part of the DOS can be correctly derived from the truncated energy dependence of nuclear inelastic scattering using the renormalized recoil energy. The exact renormalization coefficient, however, cannot be obtained solely from the truncated experimental data. As shown in the previous section, a good first approximation for the renormalization coefficient A_c is the ratio of the resonant atom and the molecule masses. However, this rule breaks down for large and soft molecules, where a considerable part of the motional energy could be embedded into molecular deformation.

In general, one could try to obtain a good approximation for the parameter of the effective recoil energy from the sum rules.¹⁶ Suppose we have measured the energy dependence of nuclear inelastic scattering only within the truncated energy region and we normalized it using effective recoil energy $A_c E_R$ with the arbitrary chosen coefficient A_c . Then we derive the DOS from the normalized energy spectrum. If the coefficient A_c is the correct one, the normalized spectrum and the derived DOS should obey several sum rules. First of all, according to Eq. (5) the area g_0 of the derived DOS should be equal to the chosen coefficient A_c . Second, the Lamb-Mössbauer factor f calculated from DOS should be equal to

$$f = \exp\left(-\omega_R \int_0^\infty \frac{d\omega}{\omega} g(\omega) \frac{1 + \exp(-\beta\omega)}{1 - \exp(-\beta\omega)}\right) = 1 - S_0, \quad (15)$$

where S_0 is the area of the inelastic part of the normalized truncated spectrum. Furthermore, one can also consider the sum rules for the higher-order moments. Proceeding similar to Eq. (5), we obtain

$$\begin{aligned} \int_{-\infty}^{\infty} d\omega \omega^2 S(\omega) &= (g_0 \omega_R)^2 + \omega_R \int_0^\infty d\omega \omega g(\omega) \frac{1 + \exp(-\beta\omega)}{1 - \exp(-\beta\omega)}, \\ \int_{-\infty}^{\infty} d\omega \omega^3 S(\omega) &= (g_0 \omega_R)^3 + \omega_R \int_0^\infty d\omega \omega g(\omega) \\ &\quad \times \left(3g_0 \omega_R \frac{1 + \exp(-\beta\omega)}{1 - \exp(-\beta\omega)} + \omega\right). \end{aligned} \quad (16)$$

These equations are a generalization of similar expressions obtained in Ref. 6 for the case of non-normalized DOS.

Strictly speaking, the equations above are fulfilled for any arbitrarily chosen coefficient A_c . On the other hand, when it is far away from the correct one, the obtained DOS acquires positive or negative artifact contributions beyond the truncated energy region. Therefore, the proper algorithm to find a good approximation for the normalization coefficient A_c would be to test the sum rules within the truncated energy region. However, our attempts to check this algorithm showed that the required accuracy can hardly be reached because these relations remain valid even for rather approximate values of A_c .

The exact value of the renormalization coefficient A_c is equal to the relative area of the lattice modes in the total DOS. Thus, the total energy spectrum should be measured at least once in the entire energy range in order to determine the area of the lattice DOS. The experimental data show that the area of the collective modes stays constant under the variable external parameters even though the shape of the DOS does change.¹⁷ Therefore, the total spectrum has to be measured once, for instance, at ambient conditions, and then the following measurements under variable external parameters of temperature, pressure, etc., can be performed only within the much narrower energy range of the truncated spectrum.

It goes without saying that the proposed approach can be generalized to any arbitrary chosen part of the energy spec-

trum around the central elastic peak, not necessarily solely to the lattice modes. Note that the analysis above does not require any specific properties of the vibrational modes within the truncated energy region. The only assumption we made was the sufficiently narrow width of the molecular peaks beyond the truncated spectrum. Therefore, the same approach can be applied for investigation of any arbitrary low-energy part of the DOS, e.g., including some molecular modes as well.

Consequently, a successful application of the approach does not mean that the derived density of states belongs exclusively to lattice phonons. The conclusion about the mode composition, however, can be done on the basis of the relative area of the studied part of the DOS. For instance, in the demonstrated example of the decamethyl ferrocene molecular crystal, the relative part of the derived DOS is sufficiently close to the ratio of the nuclear and molecular masses. This excludes the contribution of the molecular modes to the studied part of the DOS.

Furthermore, the presented analysis has even wider implications, because in practice the measured energy spectra are *always* truncated. Even if the DOS is defined within a finite-energy region, the multiphonon terms in the energy dependence of nuclear inelastic scattering expand to an infinite energy and *never* can be measured completely. Therefore, the first moment of the measured spectrum is somewhat smaller than the recoil energy of the free nucleus. Thus, the standard procedure of data processing always overestimates the normalization of the measured energy spectrum. Because of that, the area of the derived DOS within the experimental energy region is slightly higher than unity, whereas beyond this region the DOS has some small negative contributions. Similar to the case of the deliberately truncated energy spectra, these artifacts can be corrected by choosing the normalization of the first moment of the energy spectrum slightly less than the recoil energy of a free nucleus.

VII. CONCLUSIONS

We analyzed the energy dependence of nuclear inelastic scattering in a molecular crystal with well-separated lattice phonons and local molecular modes. The analysis was focused on the influence of the high-energy molecular modes on the low-energy lattice part of the energy dependence of nuclear inelastic scattering.

We demonstrated that the presence of the molecular modes does not change the shape but only rescales the lattice part of the energy dependence of nuclear inelastic scattering. Because the influence of the molecular modes is reduced to a scaling factor, the lattice part of the DOS can be properly derived even from the lattice part of nuclear inelastic scattering alone. In this case, one has to substitute the recoil energy of a nucleus by the effective recoil energy of the molecule. In a first approximation, the ratio of the recoil energies is close to the ratio of the nuclear and molecular masses. More precisely, it is given by the relative area of the lattice part in the entire DOS.

The analysis can be generalized to any arbitrary region of nuclear inelastic scattering around the elastic peak with suf-

ficiently narrow peaks beyond it. Therefore, the demonstrated property of nuclear inelastic scattering allows for a shorter measuring time in studies of various complex solids such as molecular crystals,^{11,12} proteins,^{13,14} and glasses.¹⁷ Obviously, a similar approach can be developed for inelastic neutron scattering as well.

ACKNOWLEDGMENTS

The authors are grateful to T. Asthalter and U. van Bürck for providing them with the enriched sample of decamethyl ferrocene and to H. Schottenberger for the sample preparation. The work of V.G.K. is supported by RFBR Grant No. 04-02-17363.

APPENDIX: ENHANCED THEORY OF ELASTIC PEAKS

As mentioned in the Introduction, the area of the energy dependence of nuclear inelastic scattering cannot be normalized by unity because of the saturation of the intensity of the central elastic peak. In energy representation, the saturation of the intensity of the central elastic peak is described by the saturation of incoherent scattering for a very high cross section of elastic interaction, where the yield of scattering is no longer proportional to the scattering cross section. This trivial picture becomes much more instructive when considered in a time representation. To shorten, we assume that the nuclear transition is not split by hyperfine interactions. We consider a sample of length d along the incident x-ray beam, and we suppose that the detector collects all incoherent scattering equally from the various parts of the sample. As discussed earlier,²² in the case of elastic excitation the time dependence of incoherent scattering is influenced by the coherent channel of nuclear forward scattering and, therefore, is different for various depths of the sample. It was shown²² [see Eq. (39) of the referenced paper] that the total time evolution of the elastic incoherent scattering $I_{el}(t)$ is described by

$$I_{el}(t) = f(dt_n)^{-1} \exp(-t/t_n) \int_0^d dz \exp(-\mu_e z) J_0^2([\mu_n z t/t_n]^{1/2}), \quad (\text{A1})$$

where t_n is the lifetime of the nuclear excited state, μ_e is the electronic absorption coefficient, μ_n is the nuclear absorption coefficient at the exact resonance, and $J_0(x)$ is the Bessel function of the first kind and zero order. The normalization coefficient of Eq. (A1) is chosen so that the integral of elastic incoherent scattering over time is equal to the Lamb-Mössbauer factor f for a very thin target with $d \rightarrow 0$.

In the case of inelastic excitation, the nuclear forward scattering does not appear. Neglecting the radiation trapping effect,²³ the time evolution of incoherent scattering for all phonon energies is described by a simple exponential decay with a natural lifetime. Therefore, integration over the entire energy spectrum of inelastic scattering gives the time evolution of inelastic incoherent scattering $I_{inel}(t)$ as

$$I_{inel}(t) = (1-f)(dt_n)^{-1} \exp(-t/t_n) \int_0^d dz \exp(-\mu_e z). \quad (\text{A2})$$

First, let us consider two cases where measurements are performed with the sample of a very small thickness or in a very short time interval t after a prompt pulse of synchrotron radiation. In both these cases we can substitute the Bessel function in Eq. (A1) by unity. Then the time evolutions of both elastic and inelastic parts of incoherent scattering are described by the same time dependence. The balance between the elastic and inelastic fractions of incoherent scattering is fulfilled; i.e., their contributions are weighted by f and $(1-f)$, respectively, as it should be for incoherent scattering by a single nucleus. Thus, the experimental data for a very thin sample or those taken in the very short time interval after the prompt x-ray pulse can be normalized by the area of the energy spectrum.

For thick samples and long observation time, however, the Bessel function in Eq. (A1) is significantly less than unity. This is connected to the speed-up effect of nuclear forward scattering in a thick sample.^{24,25} Equation (A1) shows that the same effect causes a decrease of the relative contribution of the elastic part of incoherent scattering. The time-integral yield of the elastic incoherent scattering $i_{el}(d)$ can be written as

$$i_{el}(d) = \int_0^\infty dt I_{el}(t) = (f/d) \int_0^d dz \exp(-\mu_e z - \mu_n z/2) I_0(\mu_n z/2), \quad (\text{A3})$$

where $I_0(x)$ is the modified Bessel function of the first kind and zero order. In a similar way one can obtain the time-integral yield of inelastic incoherent scattering $i_{inel}(d)$. The ratio

$$a(d) = \frac{i_{el}(d)(1-f)}{i_{inel}(d)f} = \frac{\mu_e \int_0^d dz \exp(-\mu_e z - \mu_n z/2) I_0(\mu_n z/2)}{1 - \exp(-\mu_e d)} \quad (\text{A4})$$

gives the reduction coefficient for the relative weight of elastic incoherent scattering in a thick sample.

In order to simplify expression (A4), we consider the range of the sample thickness where the electronic absorption is still negligible—i.e., $\mu_e d \ll 1$. In this case the reduction coefficient can be evaluated analytically:

$$\begin{aligned} a(d) &= \xi(p) = \frac{1}{p} \int_0^p dx \exp(-x) I_0(x) \\ &= \exp(-p) [I_0(p) + I_1(p)], \quad p = \mu_n d/2. \end{aligned} \quad (\text{A5})$$

The evolution of the reduction coefficient as a function of the dimensionless thickness parameter p is shown in Fig. 8. At $p < 2$, the reduction coefficient rapidly decreases from unity to about 0.5. The further decrease becomes slower. At high p , the reduction coefficient can be approximated as $\xi(p) \approx 0.798 p^{-1/2}$.

Figure 8 shows that even for the time-integral measurements the relative weight of elastic incoherent scattering decreases significantly with the sample thickness. According to Eq. (A1), this is caused by an accelerated decay of the primary wave field of nuclear forward scattering exciting the nuclei in the thick sample. In practice, the measurements of inelastic scattering are started not at zero time but some nanoseconds after the prompt pulse of synchrotron radiation. This leads to a higher reduction of the relative weight of the elastic peak in the energy spectrum of nuclear inelastic scattering.

The time integral of elastic incoherent scattering from a particular depth z in Eq. (A3) can also be obtained in the energy representation as an integral of nuclear incoherent scattering over dimensionless frequency $w = \omega t_n$ in the vicinity of nuclear resonance:

$$\exp(-\mu_n z/2) I_0(\mu_n z/2) = \int \frac{dw}{2\pi} \frac{1}{(w^2 + 1/4)} \exp\left(-\frac{\mu_n z}{w^2 + 1/4}\right). \quad (\text{A6})$$

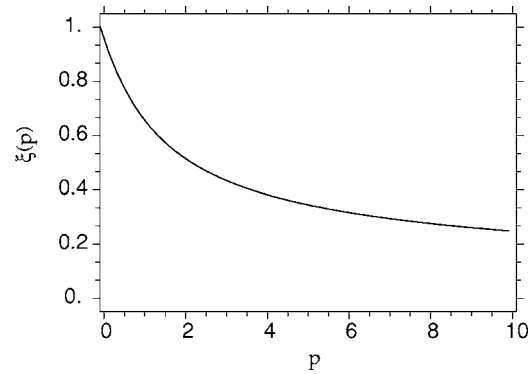


FIG. 8. The reduction coefficient of the relative weight of the elastic peak (see text for the details) as a function of the reduced thickness $p = \mu_n d/2$.

Thus, the results of the time and energy representation are consistent with each other. The exponential factor in Eq. (A6) gives a conventional interpretation of the saturation in the elastic peak intensity in terms of the saturation of incoherent scattering in a thick sample.

*URL: <http://kohnvict.chat.ru>

†Electronic address: chumakov@esrf.fr

- ¹M. Seto, Y. Yoda, S. Kikuta, X. W. Zhang, and M. Ando, *Phys. Rev. Lett.* **74**, 3828 (1995).
- ²W. Sturhahn, T. S. Toellner, E. E. Alp, X. Zhang, M. Ando, Y. Yoda, S. Kikuta, M. Seto, C. W. Kimball, and B. Dabrowski, *Phys. Rev. Lett.* **74**, 3832 (1995).
- ³A. I. Chumakov, R. Rüffer, H. Grünsteudel, H. F. Grünsteudel, G. Grübel, J. Metge, O. Leupold, and H. A. Goodwin, *Europhys. Lett.* **30**, 427 (1995).
- ⁴For a review see, e. g., A. I. Chumakov and W. Sturhahn, *Hyperfine Interact.* **123/124**, 781 (1999).
- ⁵K. S. Singwi and A. Sjolander, *Phys. Rev.* **120**, 1093 (1960).
- ⁶V. G. Kohn, A. I. Chumakov, and R. Rüffer, *Phys. Rev. B* **58**, 8437 (1998).
- ⁷W. Sturhahn and V. G. Kohn, *Hyperfine Interact.* **123/124**, 369 (1999).
- ⁸V. G. Kohn and A. I. Chumakov, *Hyperfine Interact.* **125**, 205 (2000).
- ⁹V. G. Kohn and A. I. Chumakov, *J. Phys.: Condens. Matter* **14**, 11875 (2002).
- ¹⁰A. I. Chumakov, R. Rüffer, A. Q. R. Baron, H. Grünsteudel, and H. F. Grünsteudel, *Phys. Rev. B* **54**, R9596 (1996).
- ¹¹H. Paulsen, R. Benda, C. Herta, V. Schünemann, A. I. Chumakov, L. Duelund, H. Winkler, H. Toftlund, and A. X. Trautwein, *Phys. Rev. Lett.* **86**, 1351 (2001).
- ¹²A. I. Chumakov, R. Rüffer, O. Leupold, and I. Sergueev, *Struct. Chem.* **14**, 109 (2003).
- ¹³J. T. Sage, C. Paxson, G. R. A. Wyllie, W. Sturhahn, S. M. Durbin, P. M. Champion, E. E. Alp, and W. R. Scheidt, *J. Phys.:*

Condens. Matter **13**, 7707 (2001).

- ¹⁴K. Achterhold and F. Parak, *J. Phys.: Condens. Matter* **15**, S1683 (2003).
- ¹⁵V. G. Kohn, A. I. Chumakov, and R. Rüffer, *Phys. Rev. Lett.* **92**, 243001 (2004).
- ¹⁶G. J. Lipkin, *Hyperfine Interact.* **123/124**, 349 (1999).
- ¹⁷A. I. Chumakov, I. Sergueev, U. van Bürck, W. Schirmacher, T. Asthalter, R. Rüffer, O. Leupold, and W. Petry, *Phys. Rev. Lett.* **92**, 245508 (2004).
- ¹⁸This is done in order to simplify the comparison to the initial DOS. In general, one can complete processing the truncated spectrum with the effective recoil energy. In this case, the lattice DOS will be normalized not to A_c , but to unity.
- ¹⁹R. Rüffer and A. I. Chumakov, *Hyperfine Interact.* **97-98**, 589 (1996).
- ²⁰A. I. Chumakov, R. Rüffer, O. Leupold, A. Barla, H. Thiess, T. Asthalter, B. P. Doyle, A. Snigirev, and A. Q. R. Baron, *Appl. Phys. Lett.* **77**, 31 (2000).
- ²¹Yu. T. Struchkov, V. G. Andrianov, T. N. Sal'nikova, L. R. Lyat'fov, and R. B. Materikova, *J. Organomet. Chem.* **145**, 213 (1978).
- ²²G. V. Smirnov and V. G. Kohn, *Phys. Rev. B* **52**, 3356 (1995).
- ²³A. I. Chumakov, J. Metge, A. Q. R. Baron, R. Rüffer, Yu. V. Shvyd'ko, H. Grünsteudel, and H. F. Grünsteudel, *Phys. Rev. B* **56**, R8455 (1997).
- ²⁴Yu. Kagan, A. M. Afanas'ev, and V. G. Kohn, *J. Phys. C* **12**, 615 (1979).
- ²⁵J. B. Hastings, D. P. Siddons, U. van Bürck, R. Hollatz, and U. Bergmann, *Phys. Rev. Lett.* **66**, 770 (1991).